



Characterizing drift velocity for two-phase flow using particle image velocimetry

A. A. Araoye¹, W. H. Ahmed², A. Al Sarkhi¹, O. Bamidele¹,
H. M. Badr¹ & I. H. Alsurakji¹

¹*Department of Mechanical Engineering,*

King Fahd University of Petroleum and Minerals, Saudi Arabia

²*School of Engineering, University of Guelph, Canada*

Abstract

Two-phase flow analysis is important in the design of gas and oil pipelines, the design of fuel channels in power generation industries, the prediction of heat transfer characteristics in process equipment, the operation of the gas-oil separation plants in oil production companies, the safe operation of nuclear reactors, the design of thermal desalination processes, and in many other industrial systems. The reliability or failure of these systems depends on the ability to analyze and model these types of flows. Drift velocity is an important parameter for the models used to analyse two-phase flow in vertical pipes and in the oil-water separation processes. Several studies are available for large pipe diameters. However, very few studies have been conducted in small pipe diameters and the effect of liquid phase properties has not been thoroughly investigated. In small pipe diameters, the liquid surface tension can play a significant role in determining the flow behaviour, and consequently the accuracy of the available models and correlations. In this study the drift velocity and the liquid flow characteristics for two-phase slug flow in a vertical pipe are experimentally investigated. Particle image velocimetry (PIV) along with both image pre- and post-processing techniques are adapted to determine the drift velocity, void fraction, and vorticity fields in the liquid phase.

Keywords: two-phase flow, bubbly flow, PIV.



1 Introduction

The distribution parameter and the drift velocity are two important parameters for the models used to analyse two-phase flow systems. In addition it is of great importance in the analysis of water circulation in boilers, nuclear reactors and multiphase flow modelling in vertical pipes. Several studies were reported for drift velocity in large pipe diameters covering a wide range of liquid viscosities. However, very few studies have been conducted in small pipe diameters and the effect of liquid type has not been thoroughly investigated. In small pipe diameter, the liquid surface tension may play a significant role that may affect the accuracy of the available correlations.

In order to characterize two-phase slug flow in vertical pipes, two important parameters need to be understood. These are the translational velocity and drift velocity. The translational velocity, velocity of slug units, is obtained with a closure relationship in two-phase flow mechanistic modelling. It is simply described as the summation of the bubble velocity in stagnant liquid, i.e. the drift velocity, V_d , and the maximum velocity in the slug body. Nicklin *et al.* [1] proposed an equation for translational velocity, V_t , as,

$$V_t = C_s V_s + V_d \quad (1)$$

The parameter C_s is approximately the ratio of the maximum to the mean velocity of a fully developed velocity profile. C_s equals approximately 1.2 for turbulent flow and 2.0 for laminar flow, and V_s is the mixture velocity.

Gokcal *et al.* [2] found that slug flow is a dominant flow pattern for high viscosity oil and gas flows, and the flow characteristics in this case is crucial to the design of pipelines and process equipment. He concluded that in order to improve the accuracy of slug characteristics for high viscosity oils, a model for translational velocity is required. The translational velocity is composed of a superposition of the velocity of the bubble in stagnant liquid, i.e. the drift velocity V_d , and the maximum velocity in the slug body. The research efforts, so far, have been focused on the drift velocity in horizontal pipes.

On the other hand, Wallis [3] and Dukler and Hubbard [4] claimed that there is no drift velocity for the horizontal case since gravity cannot act in the horizontal direction. However, Weber [5] and Bendiksen [6] showed that drift velocity exists for the horizontal case and the value of drift velocity can exceed the vertical case value. The drift velocity results from hydrostatic pressure difference between top and bottom of the bubble nose.

For the drift velocity in horizontal pipes, Benjamin [7] proposed the following relationship:

$$V_d = 0.542\sqrt{gD} \quad (2)$$

where the value of the drift velocity coefficient was calculated using the inviscid (potential) flow theory neglecting the surface tension and viscosity effects. The drift velocity in a horizontal slug flow is considered to be the same as the velocity of penetration of a bubble when the liquid is drained out of the pipe. The studies



of both Bendiksen [6] and Zukoski [8] have experimentally supported Benjamin [7] conclusions. Bendiksen [6] performed an experimental study for velocities of single elongated bubbles in flowing liquids at different inclination angles. He proposed the following equation for all inclination angles:

$$V_d = V_d^h \cos \beta + V_d^v \sin \beta. \quad (3)$$

where, V_d^h and V_d^v are drift velocities for horizontal and vertical flows, respectively.

Also, Zukoski [8] experimentally investigated the effects of the liquid viscosity, surface tension and pipe inclination on the motion of single elongated bubbles in a stagnant liquid for different pipe diameters. He also found that the effect of viscosity is negligible on the drift velocity for $Re = V_d \rho D / \mu > 200$. The lower values of drift velocity in horizontal pipe were due to changing the pipe diameter and not due to changing the liquid viscosity or surface tension thus the Eötvös number ($Eu = \rho D^2 g / \sigma$) was changed. The viscosities for those values were not reported.

Over the years, the measurement of two-phase flow properties such as void fraction, phase velocities, vortices, induced turbulence, have been carried out with various techniques such as Impedance Capacitance, hot-wire anemometry, Laser Doppler Velocimetry, Planar Doppler Velocimetry and Particle Image Velocimetry (PIV). PIV is relatively a new non-intrusive, optical measurement technique which allows measurement of instantaneous velocity of single- and multi-phase flows in two and three components. Its non-intrusive characteristic makes it suitable for high speed flow with shocks, boundary layer measurements in both laminar and turbulent flows. PIV enables qualitative determination of the instantaneous velocity in the entire flow field with high spatial resolution which makes it ideal for studying the flow structure in unsteady flows [9] compared to single point measurement capability of conventional measuring devices. The reliability, accuracy and applicability to any optically accessible flow made the PIV one of the relevant diagnostic tools in both industries and research [9]. It should be noted that the numerous advantages portrayed by the PIV technique are also accompanied with some challenges. One of the most challenging tasks is related to the stringent measures in obtaining reliable results such as selection of seeding particles with matching densities to the continuous phase. It measures only two velocity components with the tendency of the third components hindering the accuracy of results. The use of Stereoscopic PIV approach alleviates this as it allow for recording the instantaneous 3-D velocity vectors in the entire flow field.

Single phase flows such as air flow over a solid body or internal flow in pipes require less stringent measures in using PIV than multiphase flows because the latter poses problems such as attenuation of light sheets by densely seeded flows, velocity differences associated with each flow phase. The complexity encountered in multiphase flows is brought about by the interaction between the phases involved like gas-liquid, liquid-liquid, solid-liquid phases. Flow rate, bubble sizes and internal two-phase flow structure influences the process of surface flow generation and bubble parameters [10]. PIV analysis of multiphase flows requires



the use of light sheet optics and separation of the phases (continuous and dispersed) in order to extract the reliable information about the separate phases as well as the interaction between these phases. The multiphase concept has led to various PIV techniques which basically involve improved lighting and image acquisition and development of algorithms to provide information on phase separation, size and orientation of dispersed phase and turbulence induced by dispersed phase.

A study by Liu *et al.* [10] to determine the liquid flow velocity and turbulence generated by bubbles rising through stagnant liquids were developed using PIV. The bubbles were generated using a bubble generator with various frequencies of bubble formation. Bubbles travel upward in three different trajectories, varying from one- to three-dimensional mode as liquid viscosity reduces. Different bubble motions found to lead to different instantaneous liquid velocity fields, turbulent intensity and Reynolds stresses. Also, as the bubbles rise, a complex liquid flow field consists of vortices and cross flows is observed.

It should be noted that PIV measurements are mainly based on compromises between properties like better reflection of light (large tracer particles) and the need for tracer particles to follow the flow field (small light particles), short duration of illumination to avoid out-of-plane drift and long duration for sufficient resolution of images, distribution of tracer particles and image density method of storage of images either single frame/multiple exposure or multiple frames/single exposure [12]. This study is focused on digital PIV analysis of gas–liquid two-phase flow by an improved method of combining Phantom Camera Suite (PCC) with Dantec software. The PCC is used for determining the characteristic of the disperse phase in order for the analysis to be carried out on the Dantec software.

2 Experimental setup and data processing

The schematic diagram of the setup is shown in Figure 1. The setup consists of a transparent 25.4 mm inside diameter pipe, ray-power continuous wave laser, a speed-sense 9020 CCD phantom camera with 1600x1280 pixels and 8-bit resolution, and an Omega-flex dosing pump with flow rate ranges between 28–800 mL/min. Additionally, a Phantom Camera Control application (PCC studio) and Dantec Dynamics Studio software were used for image recording and PIV analysis respectively. The camera was positioned at right angle to the laser portion to avoid off-axis recording of images. The camera intensity calibration (also known as camera section reference) was performed at 1630x1200 resolution, sample rate of 200 fps with the exposure time set at maximum value. Bubbles were introduced from the bottom of the vertical pipe and the resolution and sample rate were adjusted to achieve the best images of the flow. Hollow Glass Sphere (HGS) seeding particles of an average sizes equal to 10 μm are used for the present measurements. Bubbly flow at different flow rates were observed and the data was recorded at a resolution of 498x1200 pixels, sample rates 800–1000 fps over 30 s duration and the corresponding pressure head were measured.

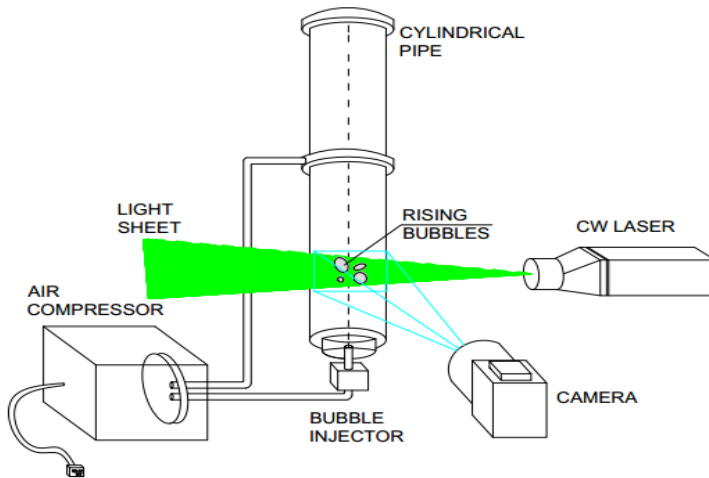


Figure 1: Schematic of the experimental set-up.

Using the PCC studio, the calibration and scaling were done to determine the bubble rise velocity and the velocity vector of liquid around the bubbles. In order to speed the image analysis, a sequence program was developed as shown in Figure 2. In this program, image pre-processing is performed to enhance the quality of the images using background subtraction and image balancing. Also, the background noise was eliminated in order to reduce the non-uniformity of illumination. An adaptive correlation scheme was used to determine velocity vectors. This scheme contains the algorithms required for image processing from cross-correlation, vector validation to image post-processing in order to achieve reliable vector maps. Cross-correlation was carried out by specifying the final interrogation areas (IA) as 32×32 pixels with 3 refinement steps, 50% horizontal and vertical overlap and Gaussian window function to remove small noise due to cyclic nature of FFT. Vector validation was achieved by setting stringent conditions like peak to height ratio to 1.2 in the peak validation algorithm to identify spurious vectors. This was combined with local neighborhood validation that replaces the spurious vectors based on the interpolation from the surrounding vectors. The IA offset was adopted to obtain accurate velocity from the mean displacement vectors by a three-point symmetric algorithm (Central difference offset).

It is very important to mention that a background subtraction is performed for image processing in the present study in order to minimize the effects of laser flare. The background reference image can be an image of the field without seeding particles. Also it can be the average of the acquired raw images with the minimum intensity. Moreover, a high pass filter to remove low frequency background variation or noise is also used. In addition, a threshold is used to obtain balanced images. This is done by utilizing a high pass filter. On the other hand, a low pass filter to remove high frequency noise due to pixel anomalies or camera shot noise is also used.

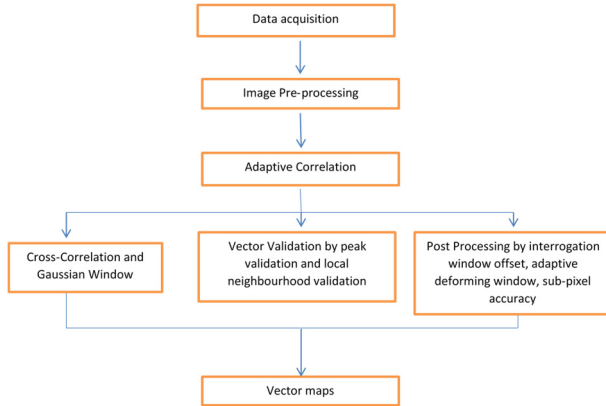


Figure 2: Sequence of the PIV analysis.

In PIV analysis of multiphase flows, the phase separation can be done either through optical or digital image processing. Phase separation is based on utilizing the distinguishing features of the phases such as particle image size and brightness, fluid dynamics or wavelength of reflected light [11]. In this study, a digital method is used utilizing median filtering. In this method, image masking which is used to distinguish phases by identifying the disparity in particle sizes and brightness. The image evaluation in PIV is carried out by dividing each image map (continuous phase in multiphase flow) into IA with sizes depending on desired accuracy, resolution and quality of the image maps. The peak displacement vector of each IA is determined through statistical techniques realized digitally using Fourier algorithms.

A masking technique adopted as suggested by Gui and Merzkirch [13] in order to differentiate between the sizes of seeding particles in continuous phase and dispersed phase (bubbles) and consequently distinguish between the recorded signals of each phase. This was done by setting a predetermined threshold value based on grayscale pixel value which wipes out the images of the phase with a color code in the lower or the higher range. The remaining pixels are identified as the second phase using the Minimum Quadratic Difference (MQD) approach. The MQD determines the displacement (m,n) of an ensemble over a certain time duration. The method is applied separately to each phase by using the conditions above or below the predetermined threshold frequency as explained in equation 4.

$$\text{MQD}(m, n) = \frac{1}{MN} \sum_{i=1}^M \sum_{j=1}^N [g_1(i, j) - g_2(i + m, j + n)]^2 \quad (4)$$

The masks were defined for two images with grayscale values $g_1(i, j)$ and $g_2(i + m, j + n)$ as $\Delta_1(i, j)$ and $\Delta_2(i + m, j + n)$ respectively and their combined (mask) is defined as:

$$\Delta = \Delta_1(i, j) \cdot \Delta_2(i + m, j + n) \quad (5)$$

and superimposed on the MDQ to establish the signals generated from each phase by representing the quadratic difference as:

$$D_B(m, n) = \frac{\sum_{i=1}^M \sum_{j=1}^N [g_1(i, j) - g_2(i+m, j+n)]^2 \Delta_1(i, j) \Delta_2(i+m, j+n)}{\sum_{i=1}^M \sum_{j=1}^N \Delta_1(i, j) \Delta_2(i+m, j+n)} \quad (6)$$

where

$$\Delta(i, j) = \begin{cases} 0 & \text{if pixel } (i, j) \text{ belongs to the gas phase} \\ 1 & \text{if pixel } (i, j) \text{ belongs to the liquid phase} \end{cases} \quad (7)$$

3 Results and discussion

The raw images of the two-phase bubble flow at different air injection rates are shown in Figure 3. The figure shows the changes in the flow pattern from bubble to slug flow as the air injection rates increases from 105 to 414 mL/min. Although, the analysis for each case of bubble injection rate was performed, only representative data for bubbly flow is included in this paper. Sequence of images for bubbly flow are displayed in Figure 4 and the corresponding velocity maps, streamlines and vorticity fields are also shown in Figures 5, 6 and 7 respectively.

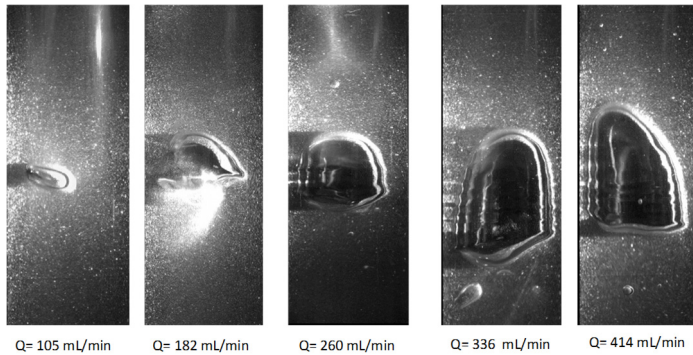


Figure 3: Flow patterns at different air injection rates.

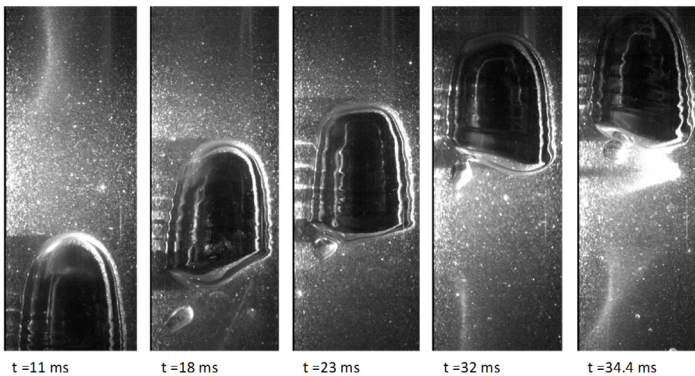


Figure 4: Position of a bubble at different times.

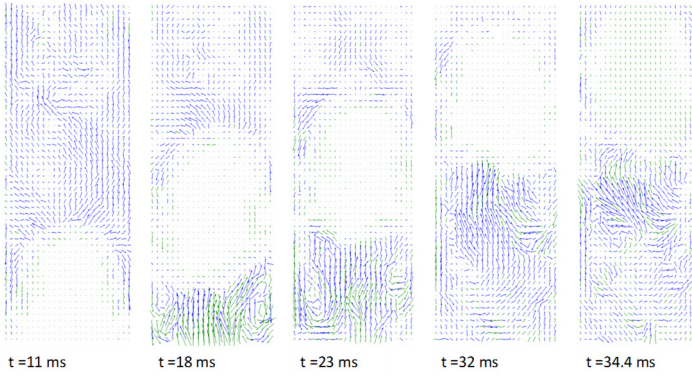


Figure 5: Velocity vector of liquid around the bubble at different times.

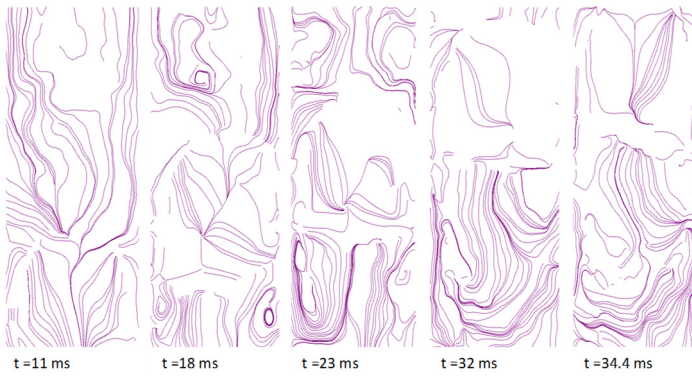


Figure 6: Streamlines in the liquid phase.

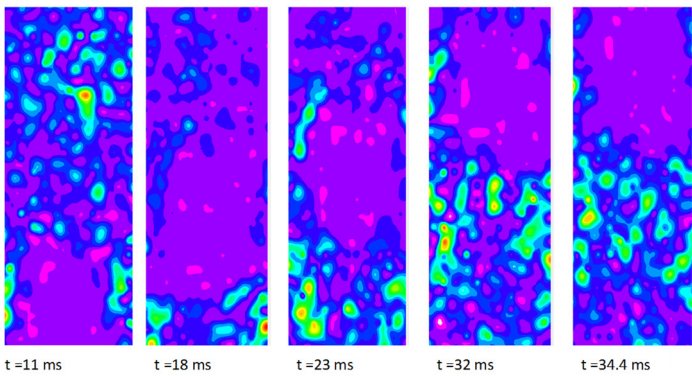


Figure 7: The vorticity map for the liquid phase.

As shown in Figure 5, the velocity vectors at the outskirts of the bubble (in the neighborhood of the bubble surface) represent the absolute local flow velocities since the camera is fixed. Accordingly, the lines tangential to these velocity vectors should not be considered as streamlines of liquid flow over the bubble. The streamlines representing flow over the bubble should be taken by a camera moving with the bubble at exactly the same velocity (Figure 6). The velocity vectors below the bubble indicate regions of vortical flow in the wake region as shown in Figure 7. If the bubble is perfectly spherical, the wake will be occupied by an axially symmetric vortex similar to that of the case of flow over a sphere. However, the shape of the bubble is not only far from being spherical or ellipsoidal but also changing as it moves upward. The volume of the bubble also changes as it moves upward because of the decrease in the hydrostatic pressure as well as the coalescence with other bubbles. Moreover, the shapes of two consecutive bubbles passing through the same section are found to be different and the velocity field over a bubble is not reproducible.

The velocity maps consist of blue and green arrow-heads which represent good vectors and substituted vectors respectively. The substituted vectors replace spurious vectors which are usually caused by insufficient particle-image to be paired, out-of-plane loss of pairs in z -direction, and in-plane loss-of-pairs in x - y directions. Comparing the image maps with the vector maps, it is seen that most of the substituted vectors are concentrated at the bubble position while the little few bad vectors are caused by the conditions stated above. This implies that masking technique will drastically reduce the number of bad vectors and ensure more accurate results.

As shown in Figure 6, the streamline maps portray the flow induced by the bubble in the stagnant water by connecting the tangents of the velocity vectors of the tracer particles. It can be observed that the streamlines are denser in the region surrounding the bubble. On the other hand, the vorticity maps presented in Figure 7 show the vorticity variation in z -direction and its effects are more in the red-yellow-green spots near the bubble position. Also, it is observed that the stagnant liquid is represented by large spaces between the streamlines. These spaces are reduced and the streamlines appears more disjointed as the velocity increases. The images were calibrated using PCC studio adjusting the pipe diameter to a scale of 0.063 mm/pix and the measurement function is adjusted in order to determine the bubble drift velocity. Five different positions of a bubble in different frames were used to calculate the bubble average velocity at displacements with respect to reference frame. Figure 8 shows the average drift velocity of bubbles at different air flow rates.

4 Conclusions

The present study showed how the PIV can be used to measure the drift velocity for gas-liquid two-phase flows. The bubble velocity, instantaneous liquid flow velocities, streamline and vorticity fields for bubbly flow were obtained utilizing a data processing algorithm for masking integrated with Dantec Dynamic studio



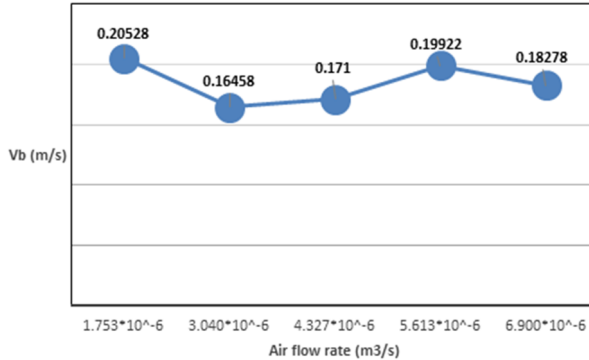


Figure 8: Drift velocity at different air injection flow rates.

software. It should be concluded that an improvement to the liquid flow field data is obtained by integrating a robust masking algorithm for the moving bubbles in order to analyze the two phases separately. This ensures achieving more accurate results by reducing the number of spurious vectors and enable determination of flow characteristics at the interphase.

Acknowledgement

The authors would like to acknowledge the support provided by the deanship of scientific research at King Fahd University of Petroleum and Minerals for funding this work through project No. FT131007.

References

- [1] Nicklin, D. J., Wilkes, J. O., and Davidson, J. F., "Two-Phase Flow in Vertical Tubes," *Trans. Inst. Chem. Eng.*, 40, pp. 61-68, 1962.
- [2] Gokcal, B., Wang, Q., Zhang, H. Q., and Sarica, C., "Effects of High Oil Viscosity on Oil-Gas Flow Behavior in Horizontal Pipes," SPE 102727, Presented at the 2006 SPE Annual Technical Conference and Exhibition, San Antonio, TX, September 24-27, 2006.
- [3] Wallis, G. B., "One Dimensional Two-Phase Flow," McGraw-Hill, New York 1969.
- [4] Dukler, A. E., and Hubbard, M. G., "A Model for Gas-Liquid Slug Flow in Horizontal and Near-Horizontal Tubes," *Ind. Eng. Chem. Fundam.*, 14, pp. 337-347, 1975.
- [5] Weber, M. E., "Drift in Intermittent Two-Phase Flow in Horizontal Pipes," *Can. J. Chem. Eng.*, 59, pp. 653-663, 1978.
- [6] Bendiksen, K. H., "An Experimental Investigation of the Motion of Long Bubbles in Inclined Tubes," *Int. J. Multiphase Flow*, 10, pp. 467-483, 1984.
- [7] Benjamin, T. B., "Gravity Currents and Related Phenomena," *J. Fluid. Mech.*, 31(2), pp. 209-248, 1968.

- [8] Zukoski, E. E., "Influence of Viscosity, Surface Tension, and Inclination Angle on Motion of Long Bubbles in Closed Tubes," *J. Fluid Mechanics*, 25(4), pp. 821-837, 1966.
- [9] Feng-Chen, K. Li, "Particle Image Velocimetry Techniques and its Applications in Multiphase Systems," *Adv. in Chem. Eng.*, 37, 2009.
- [10] Liu, Z., Zheng, Y., Jia, L., and Zhang, O., "Study of bubble induced flow structure using PIV," *Chemical Engineering Science*, 60, 3537-3552, 2005.
- [11] Saarenrinne, P., Honkanen, M., Pärssinen, T., and Eloranta, H., "Digital Imaging and PIV methods in Multiphase flows," Institute of Energy and Process Engineering Report 176, Tampere University of Technology, Finland, 2004.
- [12] Sanchez-Foreroa, D. I., Silva, J. L., Silvab, M. K., Bastosb, J. C. S. C., and Moria, M., "Experimental and Numerical Investigation of Gas-Liquid flow in a Rectangular Bubble Column with centralized Aeratin Flow pattern," *Chem. Eng. Trans.*, 32, pp. 1561-1566, 2013.
- [13] Gui, L., and Merzkirch, W., "Phase-Separation of PIV measurements in Two-Phase Flow by applying a Digital Mask Technique," *Eur. Res. Community Flow Turbulent Combustion*, 30, pp. 45-48, 1996.

